Controllable spontaneous emission spectrum in an artificial giant atom: Dark lines and bound states

Yiying Yan[1,*] and Zhiguo Lü[2,†]

[1]*Department of Physics, School of Science, Zhejiang University of Science and Technology, Hangzhou 310023, China*

[2]*Key Laboratory of Artificial Structures and Quantum Control (Ministry of Education), School of Physics and Astronomy, Shanghai Jiao Tong University, Shanghai 200240, China*

(Received 21 September 2023; accepted 12 February 2024; published 19 March 2024)

We study the spontaneous emission spectra of a few-level giant atom strongly coupled to a one-dimensional waveguide by employing variational and analytical approaches, which are beyond the rotating-wave approximation and the Markovian approximation. We show that the interference effects due to the multiple coupling points result in dark lines in spontaneous emission spectra of either two-level or three-level giant atoms regardless of whether there is a bound state or not. We illustrate that the generation of dark lines depends on the distance between the coupling points and their number. In the absence of a bound state, the dark lines can be used to suppress emission at a certain frequency in the spectrum. In the presence of a bound state, the total intensity of the emission spectrum can be significantly suppressed. The present results offer the possibility of control over the spontaneous emission with the dark lines due to the destructive interference in giant atoms.

DOI: 10.1103/PhysRevResearch.6.013301

I. INTRODUCTION

Excited atoms experience the so-called spontaneous decay due to the fluctuation of the vacuum, a transition from a higher state to a lower state accompanied by the emission of a photon, which plays a fundamental role in quantum optics [1]. Such phenomena have been mainly explored along two routines. One is concerned with the spontaneous emission of a single few-level quantum emitter in different kinds of radiation reservoirs, e.g., a free space or a structured vacuum. Several interesting effects have been found, e.g., the spontaneous-emission cancellation and Purcell effects [2–5]. The other is the collective effects of the spontaneous emission from multiple emitters. Along this routine, superradiance and subradiance are discovered [6–12]. In addition, the control over spontaneous emission to inhibit it when it is not desired or concentrate it into useful forms plays a fundamental role in the applications of photonic devices [13].

Most of the previous studies use the dipole approximation, where the atom is treated as a pointlike particle due to its size being much smaller than the wavelength of the photon. Recent experiments report that the dipole approximation despite being valid for natural atoms does not necessarily hold for a kind of artificial atoms [14–17], which couple to a radiation reservoir at multiple coupling points and are named "giant" atoms. Such atoms can be physically realized or simulated in various systems, e.g., superconducting artificial atoms coupled to a meandered transmission line or surface acoustic wave [14–18], cold atoms [19], and optical waveguides [20]. Moreover, the level structure of the artificial atom can be engineered to form a simple two-level system or a three-level system of ladder type, V type, Λ type, or even Δ type and ∇ type [21]. Giant atoms are found to have a number of unique features, for instance, a frequency-dependent decay rate and Lamb shift [22], non-Markovian retardation effects and nonexponential decay [15,23–29], the formation of a bound state in the continuum [30–32], nonreciprocal single photon scattering [33–38], realization of decoherence-free interaction [39,40], and the generation of entanglement [41–44]. Among these, the frequency-dependent emission rate, the nonexponential decay, and the formation of bound states imply a strong modification of the spontaneous emission. Very recently, the study of giant atoms has been extended to an ultrastrong coupling regime of light-matter interaction, which is beyond the rotating-wave approximation (RWA) [45,46].

So far much effort has been devoted to the modification of the spontaneous decay dynamics in giant atoms, which results from the interference effects due to the field propagating across multiple coupling points [15,23,32]. The impact of such interference effects on the spontaneous emission spectra is however rarely comprehensively explored in a strong-coupling regime where the decay rates of artificial atoms become a considerable fraction of their transition frequencies. In such a regime, the artificial atom can emit photons into a wide range of frequency modes. This raises the question of whether one can control the spontaneous emission spectrum with the giant-atom interference effects. Particularly, it is rarely explored how the formation of bound states alters the spontaneous emission spectra. It is therefore interesting to

*yiyingyan@zust.edu.cn
†zglv@sjtu.edu.cn

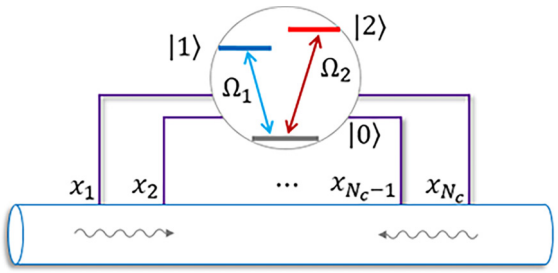

FIG. 1. Schematic representation of a V-type three-level giant atom coupled to a one-dimensional transmission line at multiple connection points x_m ($m = 1, 2, \ldots, N_c$). Ω_j ($j = 1, 2$) denotes the transition frequencies between the excited state $|j\rangle$ and ground state $|0\rangle$. When the transition between state $|2\rangle$ and ground state $|0\rangle$ is eliminated, the giant atom becomes a two-level system with transition frequency Ω_1.

revisit the spontaneous emission spectrum in the context of a giant artificial atom in a strong-coupling regime.

In this work, we study the spontaneous emission spectra of a few-level giant atom strongly coupled to a one-dimensional waveguide by using both numerical and analytical methods that are beyond the RWA and the Markovian approximation. In contrast with the previous works, we focus on the generation of dark lines in the emission spectra due to the destructive interference. By making use of a unitary transformation [47–51], we derive a transformed RWA (TRWA) Hamiltonian for a V-type three-level giant atom, which makes it feasible to numerically or analytically calculate the dynamics and emission spectrum. A steady-state emission spectrum is analytically obtained in the absence of bound states. A time-dependent variational approach with the multiple Davydov D_2 (multi-D_2) ansatz is applied to numerically calculate the spontaneous dynamics and emission spectra of a giant atom [52–55], which is used to benchmark the TRWA method. Assuming that the coupling points are equidistant, we illustrate that the interference effects arising from the multiple coupling points make it possible to suppress spontaneous emission at a certain emission frequency even in a two-level giant atom. The decay dynamics of the excitation is found to be exotic under the conditions of the spontaneous-emission suppression. We further examine the influence of the formation of bound states on the emission spectrum from a two- and three-level giant atom and find that the total intensity of the spontaneous emission spectrum can be significantly suppressed. Present results offer the possibility of control over the spontaneous emission with the dark lines due to the destructive interference in giant atoms.

II. MODEL AND METHODS

We consider a V-type three-level giant atom strongly coupled to a one-dimensional waveguide, the schematic representation of which is shown in Fig. 1. The whole system is described by the Hamiltonian ($\hbar = 1$)

$$H = H_{\rm A} + H_{\rm R} + H_{\rm I}, \tag{1}$$

where $H_{\rm A}$ is the free Hamiltonian of the atom and reads

$$H_{\rm A} = \sum_{j=0}^{2} \Omega_j |j\rangle\langle j|, \tag{2}$$

with Ω_j and $|j\rangle$ the bare energy and jth state of the atom, respectively. Throughout this work, the ground-state energy is set as $\Omega_0 = 0$. In this context, Ω_j ($j = 1, 2$) are the bare transition frequencies between excited and ground states. $H_{\rm R}$ is the free Hamiltonian of the field in the waveguide and reads

$$H_{\rm R} = \sum_k \omega_k b_k^\dagger b_k, \tag{3}$$

where b_k ($b_k^\dagger$) is the bosonic annihilation (creation) operator and ω_k is the frequency. k is the wave number, which can be either negative or positive and characterizes the right and left propagation of photons in the waveguide. A linear dispersion relation is used in this work, $\omega_k = v_g|k|$, where v_g is the velocity of photons. $H_{\rm I}$ describes the position-dependent interaction between the giant atom and the field, which reads

$$H_{\rm I} = \frac{1}{N_c} \sum_{m=1}^{N_c} \sum_k \frac{\lambda_k}{2} (b_k e^{ikx_m} + b_k^\dagger e^{-ikx_m}) L, \tag{4}$$

where N_c is the total number of coupling points, x_m are the coordinates of coupling points, and L is a transition operator of the V-type atom,

$$L = \sum_{j=1}^{2} r_j (|j\rangle\langle 0| + |0\rangle\langle j|) \equiv \sum_{j=1}^{2} V_j, \tag{5}$$

with r_j being matrix elements. The dimensionless quantities r_j ($j = 1, 2$) describe the relative coupling strengths of two transitions in the V-type three-level system driven by the vacuum field in the waveguide. If one of r_j is vanishing, the atom becomes a two-level system. $\lambda_k = \lambda_{-k}$ are the coupling constants, which characterize the dissipation through spectral density functions. In this work, we consider an Ohmic spectral density function

$$J(\omega) = \sum_k \lambda_k^2 \delta(\omega - \omega_k) = 2\alpha\omega\Theta(\omega_c - \omega), \tag{6}$$

where α is a dimensionless coupling constant, $\Theta(\cdot)$ is the Heaviside function, and ω_c is the cutoff frequency.

The present model can be physically realized in the context of circuit-QED setups, namely, a two-level or three-level superconducting artificial atom couples to a meandered one-dimensional transmission line [16,17,22], which allows the control of the distance between the coupling points. In addition, such a circuit-QED system allows the realization of strong and ultrastrong light-matter coupling regimes [56–58]. The limitation of this proposal is that the number of coupling points cannot be very large [22].

A. Transformed rotating-wave approximation

To go beyond the weak-coupling regime as well as the RWA, a unitary transformation is applied to the Hamiltonian [47–51],

$$H' = e^S H e^{-S}, \tag{7}$$

where S is the generator,

$$S = \sum_k \sum_{j=1}^{2} \frac{\xi_{kj}}{2\omega_k} (\bar{\lambda}_k^* b_k^\dagger - \bar{\lambda}_k b_k) V_j, \tag{8}$$

with $\xi_{kj} = \omega_k/(\omega_k + \Omega_j)$ and

$$\bar{\lambda}_k = \frac{\lambda_k}{N_c}\sum_{m=1}^{N_c} e^{ikx_m}. \tag{9}$$

Similar to a "small" atom case [47–51,59], we can derive a TRWA Hamiltonian $H' \approx H_0' + H_1'$. The effective free Hamiltonian reads

$$H_0' = \sum_{j=0}^{2}\tilde{\Omega}_j|j\rangle\langle j| + \sum_k \omega_k b_k^\dagger b_k, \tag{10}$$

with the renormalized frequencies of the atom given by

$$\tilde{\Omega}_0 = -\sum_k\sum_{i=1}^{2}|\bar{\lambda}_k|^2 r_i^2\frac{1}{4(\omega_k+\Omega_i)}, \tag{11}$$

$$\tilde{\Omega}_j = \Omega_j - r_j^2\sum_k|\bar{\lambda}_k|^2\frac{\omega_k+3\Omega_j}{4(\omega_k+\Omega_j)^2}\quad(j=1,2). \tag{12}$$

From the above expressions, we note that $\tilde{\Omega}_j < \Omega_j$.

The effective interaction Hamiltonian is given by

$$H_1' = \sum_k\sum_{j=1}^{2}(\tilde{\lambda}_{kj}b_k|j\rangle\langle 0| + \text{H.c.}) - W(|1\rangle\langle 2| + |2\rangle\langle 1|), \tag{13}$$

where

$$\tilde{\lambda}_{kj} = \frac{r_j\Omega_j\bar{\lambda}_k}{\omega_k+\Omega_j} \tag{14}$$

is the effective coupling constant and

$$W = \frac{r_1 r_2}{8}\sum_k|\bar{\lambda}_k|^2\frac{2\omega_k+3(\Omega_1+\Omega_2)}{(\omega_k+\Omega_1)(\omega_k+\Omega_2)} \tag{15}$$

is the indirect coupling strength between two excited states. Importantly, we note that $|\tilde{\lambda}_{kj}| < |r_j\bar{\lambda}_k|$, that is, the effective coupling constants become smaller than the bare ones, which makes it possible that the TRWA Hamiltonian is valid in a strong-coupling regime while the usual RWA Hamiltonian breaks down.

In a single-excitation case, the time-dependent Schrödinger equation in the transformed frame can be solved by the following ansatz:

$$|\Psi'(t)\rangle = \sum_{j=1}^{2}a_{j0}|j,\mathbf{0}\rangle + \sum_k a_{0k}|0,1_k\rangle, \tag{16}$$

where a_{j0} and a_{0k} are time-dependent coefficients. Their equations of motion read

$$i\dot{a}_{10} = \tilde{\Omega}_1 a_{10} - Wa_{20} + \sum_k\tilde{\lambda}_{k1}a_{0k}, \tag{17a}$$

$$i\dot{a}_{20} = -Wa_{10} + \tilde{\Omega}_2 a_{20} + \sum_k\tilde{\lambda}_{k2}a_{0k}, \tag{17b}$$

$$i\dot{a}_{0k} = (\tilde{\Omega}_0+\omega_k)a_{0k} + \sum_{j=1}^{2}\tilde{\lambda}_{kj}^* a_{j0}. \tag{17c}$$

These equations can be numerically or analytically solved with the initial condition

$$\begin{aligned}|\Psi'(0)\rangle &= e^S|\Psi(0)\rangle\\ &\approx\sum_{j=1}^{2}\left(c_j - \frac{1}{2}\sum_k g_{kj}\sum_{i=1}^{2}g_{ki}^* c_i\right)|j,\mathbf{0}\rangle\\ &\quad+\sum_k\sum_{j=1}^{2}c_j g_{kj}^*|0,1_k\rangle,\end{aligned} \tag{18}$$

where

$$g_{kj} = \frac{r_j\bar{\lambda}_k}{2(\omega_k+\Omega_j)} \tag{19}$$

and

$$|\Psi(0)\rangle = \left(\sum_{j=1}^{2}c_j|j\rangle\right)\otimes|\mathbf{0}\rangle \tag{20}$$

is an initial state of the whole system in the laboratory frame with c_j the coefficients and $|\mathbf{0}\rangle$ the multimode vacuum state.

On solving the equations of motion, we can calculate populations of state $|j\rangle$ in the laboratory frame with the quantities in the transformed frame, i.e., a_{j0} and a_{0k}. Specifically, the excited-state population is given by ($j = 1, 2$)

$$\begin{aligned}\rho_{jj}(t) &= \left(1-\sum_k|g_{kj}|^2\right)|a_{j0}|^2 + 2\,\text{Re}\left(\sum_k g_{kj}a_{j0}^* a_{0k}\right)\\ &\quad+\sum_k|g_{kj}|^2\sum_p|a_{0p}|^2 - \text{Re}\left(\sum_k g_{k1}g_{k2}^* a_{10}^* a_{20}\right).\end{aligned} \tag{21}$$

Similarly, the number of photons occupying the mode k can also be evaluated as

$$\begin{aligned}N(k,t) &= |a_{0k}|^2 - 2\sum_{j=1}^{2}g_{kj}\text{Re}(a_{j0}^* a_{0k})\\ &\quad+\sum_{j=1}^{2}g_{kj}^2\left(|a_{j0}|^2 + \sum_p|a_{0p}|^2\right)\\ &\quad+2\,\text{Re}(g_{k1}g_{k2}^* a_{10}^* a_{20}).\end{aligned} \tag{22}$$

The detailed derivation of the population of the atom and the occupation number of the field is presented in Appendix A. The emission spectrum is thus defined as

$$N(\omega_k,t) = N(k,t) + N(-k,t)\quad(k>0), \tag{23}$$

which counts photon numbers at frequency ω_k and time t.

B. Time-dependent variational approach

The presented giant-atom model under consideration can be viewed as an extension of the spin-boson model. Consequently, the dynamics of the whole system can be solved by a time-dependent variational approach equipped with the multi-D_2 ansatz, which is applicable to spin-boson problems in strong-coupling regimes. The variational approach is based

on the Dirac-Frenkel variational principle [60], which is applied to solve the time-dependent Schrödinger equation in the interaction picture governed by the reservoir Hamiltonian $H_{\rm R}$,

$$\langle\delta\psi(t)|i\partial_t - \tilde{H}(t)|\psi(t)\rangle = 0, \tag{24}$$

where $|\psi(t)\rangle$ is a parametrized trial state, $\langle\delta\psi(t)|$ is the variation of the adjoint state of the trial state, and

$$\tilde{H}(t) = \exp(iH_{\rm R}t)(H_{\rm A} + H_{\rm I})\exp(-iH_{\rm R}t). \tag{25}$$

In this work, we use the multi-D_2 state [53–55],

$$|D_2^M(t)\rangle = \sum_{n=1}^{M}\sum_{j=0}^{2} A_{nj}|j\rangle|f_n\rangle, \tag{26}$$

where A_{nj} are amplitudes and $|f_n\rangle$ are the coherent states,

$$|f_n\rangle = \exp\left[\sum_k (f_{nk}b_k^\dagger - \text{H.c.})\right]|\mathbf{0}\rangle, \tag{27}$$

where f_{nk} are displacements. A_{nj} and f_{nk} are time-dependent variational parameters to be determined via Eq. (24). One readily derives the equations of motion for the variational parameters, which is a set of implicit nonlinear first-order differential equations and can be solved with the Runge-Kutta algorithm when initial conditions are specified and the frequencies ω_k and coupling constants λ_k are derived from the spectral density function [53,59,61–63].

For the Ohmic spectral density function, we use a linear discretization procedure and suppose left- and right-propagating modes contributing equally to the spectral density function. The frequency domain $[0, \omega_c]$ is divided into N_b equal segments $[\nu_{n-1}, \nu_n]$ with $\nu_n = n\omega_c/N_b (n = 0, 1, 2, \ldots, N_b)$; supposing that each segment contains one left- and one right-propagating mode, the values of λ_k and ω_k can be calculated by the following integration,

$$\begin{aligned}\lambda_n^2 = \lambda_{-n}^2 &= \frac{1}{2}\int_{\nu_{n-1}}^{\nu_n} J(\nu)d\nu \\ &= \frac{\alpha(2n-1)\omega_c^2}{2N_b^2} \quad (n = 1, 2, 3, \ldots, N_b),\end{aligned} \tag{28}$$

$$\begin{aligned}\omega_n = \omega_{-n} &= \frac{1}{2}\lambda_n^{-2}\int_{\nu_{n-1}}^{\nu_n} \nu J(\nu)d\nu \\ &= \frac{\left(n^2 - n + \frac{1}{3}\right)\omega_c}{\left(n - \frac{1}{2}\right)N_b} \quad (n = 1, 2, 3, \ldots, N_b),\end{aligned} \tag{29}$$

where $1/2$ is used to cancel out double counting. Discrete wave numbers are obtained by the dispersion relation $k_{\pm n} = \pm\omega_n/v_g$. In this work, we use identical numbers of left- and right-propagating modes, $N_b = 300$, and the total number of modes is thus $2N_b = 600$. This guarantees the convergence of variational dynamics in a time interval $[0, 1800]\omega_c^{-1}$.

The physical quantities of interest are populations of the atom and occupation numbers of photons at each mode. On obtaining the variational parameters, the former can be readily computed as

$$\rho_{jj}(t) = \left\langle D_2^M(t)|j\rangle\langle j|D_2^M(t)\right\rangle = \sum_{n,l=1}^{M} A_{lj}^* \mathcal{S}_{ln} A_{nj}, \tag{30}$$

where

$$\mathcal{S}_{ln} = \exp\left[\sum_k \left(f_{lk}^* f_{nk} - \frac{|f_{lk}|^2 + |f_{nk}|^2}{2}\right)\right]. \tag{31}$$

The photon numbers in the mode k are given by

$$\begin{aligned}N(k,t) &= \left\langle D_2^M(t)\middle|b_k^\dagger b_k\middle|D_2^M(t)\right\rangle \\ &= \sum_{n,l=1}^{M}\sum_{i=0}^{2} A_{li}^* f_{lk}^* \mathcal{S}_{ln} f_{nk} A_{ni}.\end{aligned} \tag{32}$$

In general, the variational approach gives rise to time-dependent spectra. Intuitively, one may expect that the steady-state spectrum $N(\omega_k) = \lim_{t\to\infty} N(\omega_k, t)$ can be calculated by propagating the equations of motion in a sufficiently long time. However, this is not always practical because the spontaneous decay of the atom may be very slow under certain conditions and it becomes quite numerically demanding to obtain a steady-state spectrum. We will discuss such a scenario in detail in the following.

III. RESULTS AND DISCUSSIONS

A. Analytical steady-state spectrum

The above formal calculations are not transparent. We further analytically derive the emission spectrum in the long-time limit ($t \to \infty$), which is simply obtained via the Laplace transform of Eq. (17) with the initial condition $|\Psi'(0)\rangle = |\Psi(0)\rangle$ (the influence of the unitary transformation on the initial state is neglected). First, note that $a_{j0} \to 0$ ($j = 1, 2$) as $t \to \infty$ due to the spontaneous decay of the excited states (this is not always the case and a_{j0} may be nonvanishing due to the existence of a bound state). Second, note that $g_{kj} \propto \lambda_k$ is a small quantity and $\sum_p |a_{0p}|^2 \to 1$ as $t \to \infty$ due to the conservation of the norm of the state. With such observations, it follows from Eq. (22) that, in the long-time limit, the photon number in the mode k is dominated by $|a_{0k}|^2$. The asymptotic expression of a_{0k} can be derived with the Laplace transform (see Appendix B) and yields the analytical spectrum,

$$N(\omega_k) \approx 2F(\omega_k)\frac{\lambda_k^2}{\omega_k^2}\left|\frac{r_1\Omega_1\xi_{k1}[c_1\tilde{A}_2(\omega_k) - c_2\tilde{B}(\omega_k)] + r_2\Omega_2\xi_{k2}[c_2\tilde{A}_1(\omega_k) - c_1\tilde{B}(\omega_k)]}{\tilde{A}_1(\omega_k)\tilde{A}_2(\omega_k) - \tilde{B}^2(\omega_k)}\right|^2, \tag{33}$$

where

$$\tilde{A}_j(\omega) = \omega - \tilde{\omega}_{j0} - \tilde{\Delta}_{jj}(\omega) + i\tilde{\Gamma}_{jj}(\omega), \tag{34}$$

$$\tilde{B}(\omega) = W - \tilde{\Delta}_{12}(\omega) + i\tilde{\Gamma}_{12}(\omega), \tag{35}$$

$$F(\omega) = \frac{1}{N_c^2}\sum_{m,l=1}^{N_c} e^{i\omega(x_m - x_l)/v_g}, \tag{36}$$

$$\tilde{\Delta}_{jj'}(\omega) = P\int_0^{\omega_c} \frac{r_j r_{j'}\Omega_j\Omega_{j'}F(\nu)J(\nu)d\nu}{(\omega-\nu)(\nu+\Omega_j)(\nu+\Omega_{j'})}, \tag{37}$$

$$\tilde{\Gamma}_{jj'}(\omega) = \pi\frac{r_j r_{j'}\Omega_j\Omega_{j'}}{(\omega+\Omega_j)(\omega+\Omega_{j'})}F(\omega)J(\omega), \tag{38}$$

and $\tilde{\omega}_{j0} = \tilde{\Omega}_j - \tilde{\Omega}_0$ is the renormalized transition frequency. When $|x_m - x_l| \to 0$ or $N_c = 1$, i.e., $F(\omega) = 1$, the present result coincides with the leading term of the spectrum from a "small" atom case derived with the resolvent-operator formalism [59]. The analytical result shows two direct consequences of the multiple coupling points. First, the spectrum explicitly depends on $F(\omega)$. This means that the line shape of the spectrum can be profoundly modified by tuning $|x_m - x_l|$ and/or N_c. Particularly, spontaneous-emission suppression at certain frequencies may be achieved by using the elaborately designed zeros of $F(\omega)$. Second, $F(\omega)$ can substantially modify line positions and widths of the spectrum due to its influence on $\tilde{\Omega}_j$, $\tilde{\Delta}_{jj'}(\omega)$, and $\tilde{\Gamma}_{jj'}(\omega)$. The function $F(\omega)$ reflects the interference effects arising from the multiple coupling points. The present findings imply that the spontaneous emission can be engineered with multiple coupling points via the function $F(\omega)$ and is substantially different from the typical "small" atom cases. In the following, we illustrate how the spontaneous emission is modified due to this function.

In the present giant-atom model, bound states may exist [30,32,46]. In other words, a_{j0} has a nonvanishing value in the long-time limit. In such a case, Eq. (33) cannot be applied and the analytical calculation of the spectrum becomes cumbersome. Nevertheless, we can numerically calculate the emission spectrum based on Eqs. (17) and (22).

B. Numerical results

In this section, we numerically calculate the emission spectra and dynamics by making use of the TRWA and variational methods. Additionally, we also calculate the emission spectrum with the analytical result (33) when it is applicable. Throughout this work, we set the transition element $r_1 = 1$ and the cutoff frequency $\omega_c = 5\Omega_1$. We define $l_0 \equiv v_g/\Omega_1$ as the units of distances. Moreover, we consider that the coupling points are equidistant, that is, $x_m = md$, where d is the distance between the two nearest neighboring coupling points. In such a case, we simply have the explicit form of the function $F(\omega)$, which reads [22]

$$F(\omega) = \frac{\sin^2\left(\frac{N_c\omega d}{2v_g}\right)}{N_c^2\sin^2\left(\frac{\omega d}{2v_g}\right)}. \tag{39}$$

1. Spontaneous emission suppression without bound state

We now explore how to use the zeros of $F(\omega)$ to alter the spontaneous emission. Note that given ω_E the desired frequency to be suppressed, when the distance d is given by

$$d = \frac{2\pi n v_g}{N_c\omega_E} \quad (n = 1, 2, \ldots) \tag{40}$$

and

$$d \neq \frac{2\pi l v_g}{\omega_E} \quad (l = 1, 2, \ldots), \tag{41}$$

we simply have $F(\omega_E) = 0$. We should emphasize that the second inequality (41) makes the denominator in $F(\omega)$ nonvanishing; otherwise, $F(\omega) \neq 0$ even though Eq. (40) is fulfilled.

To illustrate the suppression of the emission at frequency ω_E, we first calculate the emission spectra of a two-level giant atom by using the TRWA and variational methods. In a two-level system, there is no quantum-interference effect arising from different transitions [64]. The spectrum for a two-level giant atom can be obtained by turning off the transition $|0\rangle \leftrightarrow |2\rangle$, i.e., $r_2 = 0$. In Figs. 2(a)–2(c), we show the emission spectra characterized by the scaled photon numbers $N_b \times N(\omega_k, t)$ as a function of ω_k for $c_1 = 1$, $c_2 = 0$, $r_2 = 0$, and the three values of N_c. The parameter d is determined by Eq. (40) with $\omega_E = 0.8\Omega_1$ and $n = 1$. The TRWA numerical spectra and the variational spectra are obtained at a finite time $t = 350\Omega_1^{-1}$. The analytical result (33) yields steady-state spectra in the limit of $t \to \infty$. The TRWA and variational numerical results agree well with each other and are overall consistent with the analytical predictions despite there being additional small peaks in the former [see Figs. 2(b) and 2(c)]. Such peaks arise from the finite time evolution. On the other hand, the deviation between the TRWA numerical and analytical results can be ascribed to the fact that, in deriving the latter, the influence of the unitary transformation on the initial state has been neglected and the analytical spectrum is evaluated in the limit of $t \to \infty$. The present results confirm the validity of the TRWA treatment for a giant atom.

We now analyze the spectral features associated with the multiple coupling points. When $N_c = 1$, the spectrum reduces to a "small" atom case, which is singly peaked at about $\omega_k = 0.8\Omega_1$. The emission peak is found to be very broad, which reflects the fact that the (artificial) atom-field coupling is strong. When $N_c = 2$, the peak is replaced by a Fano-type dark line with the minimum at ω_E. Besides, there are additional minima in the spectrum due to the additional zeros of $F(\omega)$. When $N_c = 3$, the spectral profiles are similar to those in the case of $N_c = 2$. The present results confirm the profound modification to the spontaneous emission spectrum due to the function $F(\omega)$.

To explore how the function $F(\omega)$ influences the decay rate, we calculate the excited-state population by the TRWA and variational methods in Figs. 2(d)–2(f), the parameters of which are the same as Figs. 2(a)–2(c), respectively. When $N_c = 1$, the excited-state population decays into a steady value in a short time. However, when $N_c = 2$ or 3, the excited-state population quickly decays in a short time and then experiences a revival and, after that, it slowly decays. Importantly, the excited-state population does not reach a steady value at $t = 350\Omega_1^{-1}$, which is in sharp contrast with the case of $N_c = 1$. In addition, the TRWA and variational approaches are also consistent with each other in the dynamics of the system.

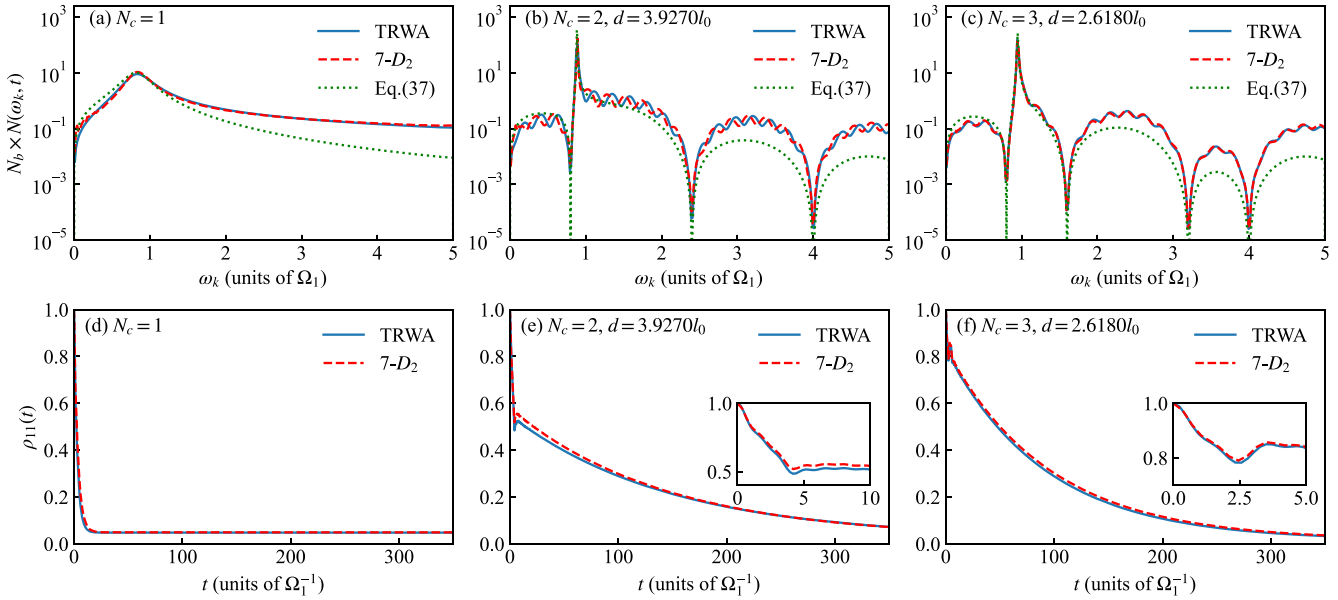

FIG. 2. (a)–(c) Emission spectrum in the two-level case obtained by multiplying $N(\omega_k, t)|_{t=350\Omega_1^{-1}}$ with $N_b = 300$ for $\alpha = 0.1$, $c_1 = 1$, $c_2 = 0$, $r_2 = 0$, $\omega_E = 0.8\Omega_1$, and three values of N_c. Distance d is determined by Eq. (40) with $n = 1$. (d)–(f) Dynamics of excited state calculated by the TRWA and variational methods for the parameters in (a)–(c).

We now study the suppression of the spontaneous emission from a V-type three-level giant atom. In Figs. 3(a)–3(c), we plot the emission spectrum for $c_1 = 1$, $c_2 = 0$, $r_2 = 1$, $\Omega_2 = 1.2\Omega_1$, $\alpha = 0.1$, the three values of N_c, and the three values of d. The TRWA and variational numerical spectra are obtained at $t = 350\Omega_1^{-1}$. Once again we see the consistency between the TRWA and variational methods, suggesting the validity of the former for a multilevel giant atom in a strong-coupling regime. We focus on the spectral features. When $N_c = 1$, i.e., the "small" atom case, there is a Fano-type dark line in the spectrum, which arises from the quantum interference between the two transitions from an upper state to a lower state [64]. When $N_c = 2$ or 3, we see that the broad spectral component in the range of $\omega_k \in (0, \Omega_1)$ is changed to a Fano-type dark line with its minimum at $\omega_E = 0.8\Omega_1$. This finding is consistent with that in the two-level case. Figures 3(d)–3(f) show the spontaneous decay dynamics for the parameters in Figs. 3(a)–3(c), respectively. When $N_c = 1$, the decay of the excited-state populations is relatively fast and there are no apparent oscillatory behaviors. However,

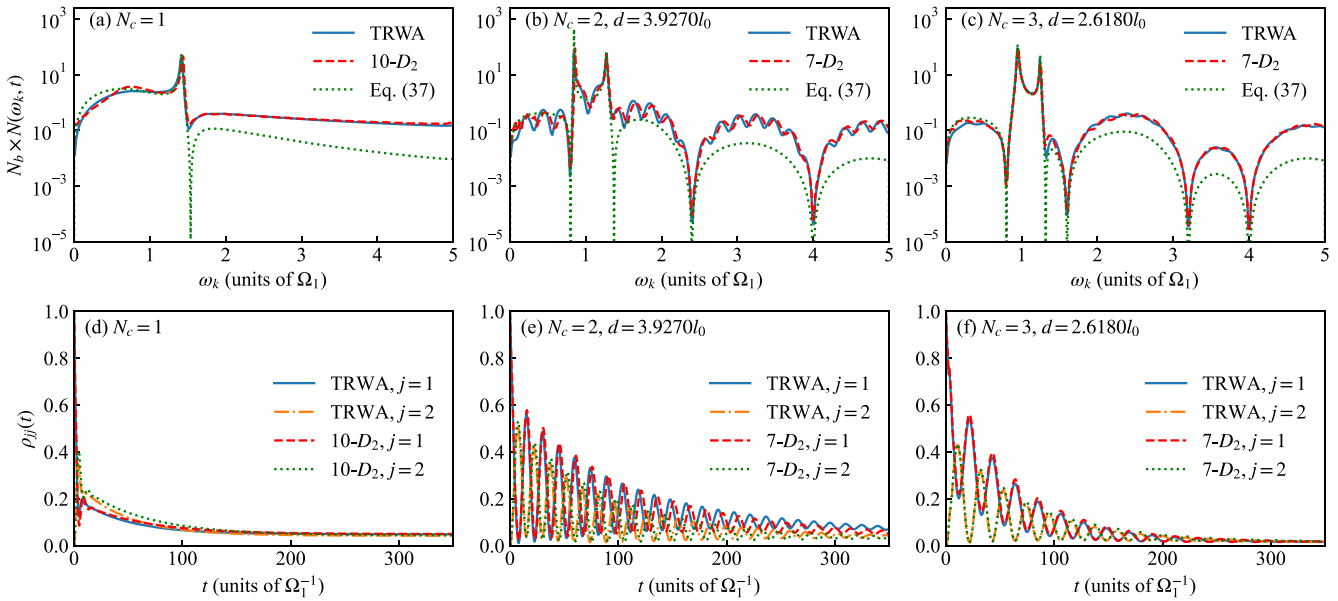

FIG. 3. (a)–(c) Emission spectrum in the three-level case obtained by multiplying $N(\omega_k, t)|_{t=350\Omega_1^{-1}}$ with $N_b = 300$ for $\alpha = 0.1$, $c_1 = 1$, $c_2 = 0$, $r_2 = 1$, $\Omega_2 = 1.2\Omega_1$, $\omega_E = 0.8\Omega_1$, and three values of N_c. Distance d is determined by Eq. (40) with $n = 1$. (d)–(f) Dynamics of excited state calculated by the TRWA and variational methods for the parameters in (a)–(c).

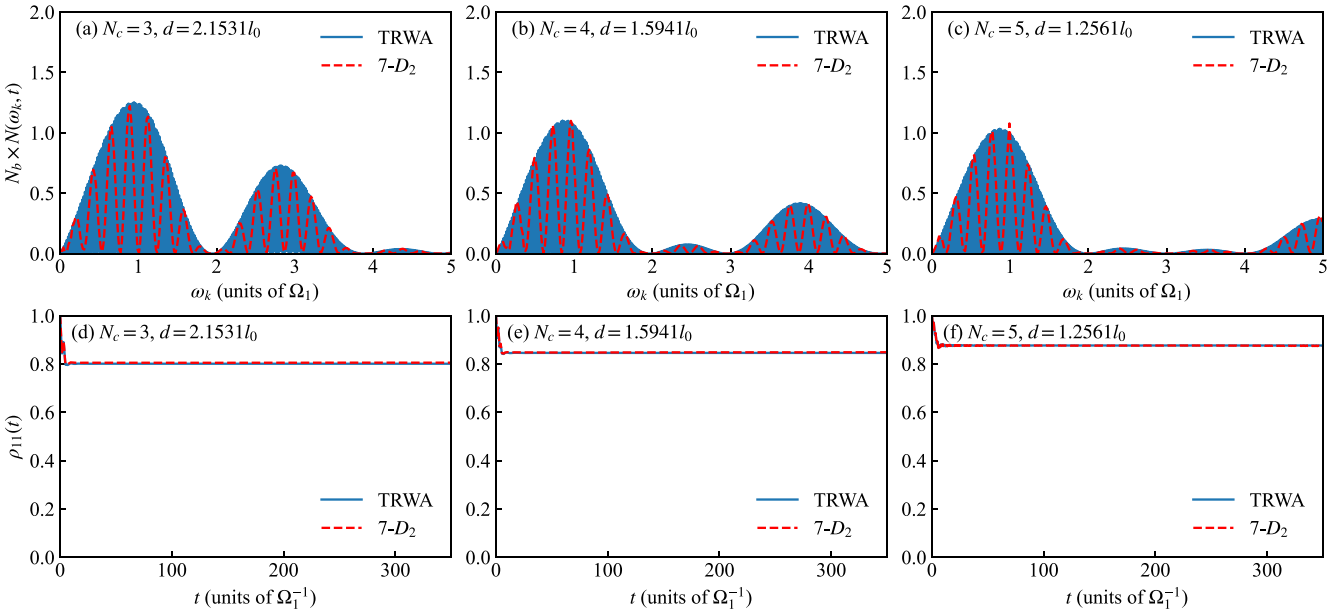

FIG. 4. (a)–(c) Emission spectrum in the two-level case obtained by multiplying $N(\omega_k,t)|_{t=350\Omega_1^{-1}}$ with N_b for $\alpha=0.1$, $c_1=1$, $c_2=0$, $r_2=0$, and three pairs of (N_c,d) given $n=1$. (d)–(f) Dynamics of excited-state population calculated by the TRWA and variational methods for the parameters in (a)–(c). $N_b=3000$ is used for the TRWA method and $N_b=300$ for the variational method.

when $N_c=2$ or 3, the populations decay relatively slowly and exhibit damped oscillations. The occurrence of the oscillations can be ascribed to the fact that the decay rate becomes smaller in the presence of the multiple coupling points and the indirect coupling between the two excited states, W, becomes much greater than the decay rate. In this scenario, the indirect coupling should be viewed as a strong coupling.

Although we just present the spectra in the case of $\alpha=0.1$, it is straightforward to verify that the dark lines due to the zeros of $F(\omega)$ also occur for other values α. That is to say, the suppression of spontaneous emission can be illustrated for other values α. On the other hand, the Ohmic parameter $\alpha=0.1$ is physically realizable in the circuit-QED setups [56], which cannot be tackled by the RWA. Present results show the possibility of achieving suppression of the spontaneous emission in a giant atom by tuning the distance d in the presence of a few coupling points, which are incorporated in the function $F(\omega)$. Although a specific form of $F(\omega)$ has been used, the present methods and analysis can be applied to an arbitrary form of $F(\omega)$. Moreover, it is possible that by designing a sophisticated configuration of multiple coupling points to realize a special form of $F(\omega)$ controls the spontaneous emission and dynamics.

2. *Spontaneous emission suppression with bound states*

We illustrate how the formation of bound states in the giant atom influences the spontaneous emission spectrum. To begin with, we consider a two-level giant atom case, i.e., $r_2=0$. In the two-level case, the excitation frequency and lifetime are determined by the following equation [30,32,46] (see Appendix B):

$$\omega-\tilde{\omega}_{10}-\tilde{\Delta}_{11}(\omega)+i\tilde{\Gamma}_{11}(\omega)=0. \tag{42}$$

Provided that there exists a bound state whose frequency is denoted by ω_B, we must have $\tilde{\Gamma}_{11}(\omega_B)=0$. The zeros of $\tilde{\Gamma}_{11}(\omega)$ can be easily achieved by choosing

$$\omega_B=\frac{2\pi n v_g}{N_c d} \tag{43}$$

and

$$\omega_B\neq\frac{2\pi l v_g}{d}. \tag{44}$$

Plugging (43) into (42), we numerically solve the equation $[\omega-\tilde{\omega}_{10}-\tilde{\Delta}_{11}(\omega)]|_{\omega=\omega_B}=0$ for the variable d for fixed N_c and n by using the bisection algorithm. In doing so, we can obtain a suitable distance d which permits the formation of the bound state.

To verify the existence of the bound state and its influence on the spontaneous emission, we use the variational approach and TRWA method to calculate the spectrum and dynamics for $\alpha=0.1$, $c_1=1$, $c_2=0$, $r_2=0$, and the three pairs of (N_c,d) given $n=1$. The emission spectra are characterized by $N_b\times N(\omega_k,t)|_{t=350\Omega_1^{-1}}$. Hereafter we use $N_b=3000$ for the TRWA calculation, while $N_b=300$ for the variational calculation (which becomes very inefficient with a large number of modes). Figures 4(a)–4(c) show that the emission spectra oscillate very fast with the variation of emission frequency ω_k, which is easily seen from the variational results. We should emphasize that the variational spectra shown are not completely converged due to the use of a relatively small number of modes. Nevertheless, we see that the two methods predict almost the same envelope of the spectra. In addition, it is worthwhile to note that the magnitude of the spectra is overall much smaller than that in the case of $N_c=1$ [see Fig. 2(a)]. This finding suggests that the total intensity of the spontaneous emission is suppressed because of the formation of bound states. Figures 4(d)–4(f) show the dynamics of the

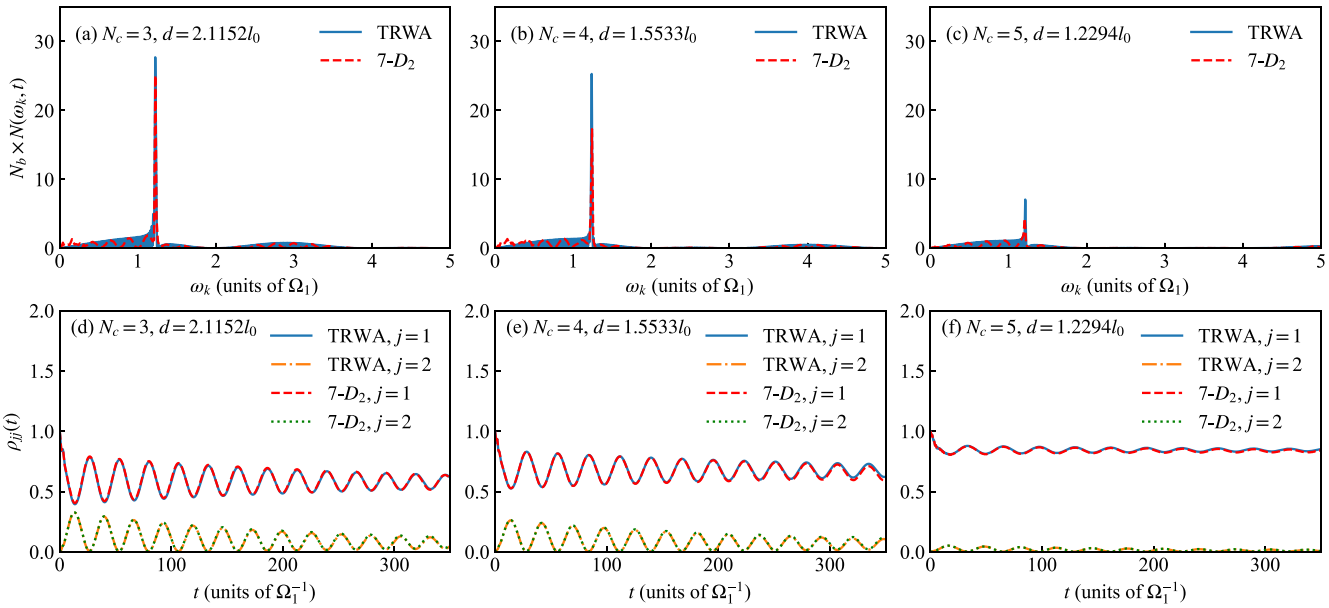

FIG. 5. (a)–(c) Emission spectrum in the three-level case obtained by multiplying $N(\omega_k,t)|_{t=350\Omega_1^{-1}}$ with N_b for $\alpha=0.1$, $c_1=1$, $c_2=0$, $r_2=1$, $\Omega_2=1.2\Omega_1$, and three pairs of (N_c,d) given $n=1$. (d)–(f) Dynamics of excited-state populations calculated by the TRWA and variational methods for the parameters in (a)–(c). $N_b=3000$ is used for the TRWA method and $N_b=300$ for the variational method.

excited-state population for the parameters in Figs. 4(a)–4(c), respectively. The TRWA and variational dynamics are consistent and converged regardless of the use of two different numbers of modes. Of particular interest, the excited-state population is found to damp in a short time and then it is trapped to a stable value, which signifies the formation of a bound state [30,32,46]. Moreover, we see that the nonvanishing value of the excited state population is enhanced by increasing N_c.

We now further illustrate the formation of bound states as well as their role in a three-level giant atom case. Note that when Eqs. (43) and (44) are fulfilled, $\tilde{\Gamma}_{jj'}(\omega_B)=0$. We search the bound-state solutions by solving the equation (see Appendix B)

$$\left\{\prod_{j=1}^{2}[\omega-\tilde{\omega}_{j0}-\tilde{\Delta}_{jj}(\omega)]-[W-\tilde{\Delta}_{12}(\omega)]^2\right\}\Bigg|_{\omega=\omega_B}=0 \tag{45}$$

for the variable d for fixed N_c and n. It is verified by using the numerical method that the equation generally has two different solutions for d. In addition, the zeros generally turn out to be the first order and thus can be obtained by the bisection algorithm.

In Figs. 5(a)–5(c), we calculate the emission spectra by using the TRWA and variational methods for $\alpha=0.1$, $c_1=1$, $c_2=0$, $r_2=1$, $\Omega_2=1.2\Omega_1$, and the three pairs of (N_c,d) given $n=1$. We see that, apart from a relatively intense narrow emission line peaked at about $\omega_k=1.2\Omega_1$, the intensity of the spectra is overall relatively small, indicating the suppression of the emission due to the formation of a bound state. The dynamics of the excited-state populations for the parameters in Figs. 5(a)–5(c) are shown in Figs. 5(d)–5(f), respectively. The TRWA and variational results are consistent with each other. It is intuitive to imagine the physical picture behind the spectra from the dynamics. Specifically, the population of the state $|1\rangle$ is partially transferred to the state $|2\rangle$ before the former evolves into a bound state. It is the spontaneous emission from the state $|2\rangle$ that results in an intense narrow peak. In addition, we see that the nonvanishing steady population of the state $|1\rangle$ can be enhanced by tuning N_c, which in turn makes the narrow peak weakened. Present results show a feasible way to modify the spontaneous emission spectra of a giant atom with a bound state.

Having considered the case of $n=1$ in Eq. (43) in the above analysis, we now show the role of n in the formation of bound states and how it influences the emission spectrum. Roughly speaking, given a fixed N_c, a larger n simply leads to a larger solution d for Eqs. (42) and (45). It follows from Eq. (39) that the function $F(\omega)$ oscillates much faster with the increasing of d. In this sense, there are more zeros of $F(\omega)$ appearing in the frequency domain $[0,\omega_c)$, which may lead to an increase in the number of the suppressed nodes of the spectral envelope where the emission intensity is almost zero. To see this, we calculate the emission spectra by using the TRWA and variational methods for $\alpha=0.1$, $c_1=1$, $c_2=0$, $N_c=3$, and $n=4$. Figures 6(a) and 6(b) show the scaled spectra $N_b\times N(\omega_k,t)|_{t=350\Omega_1^{-1}}$ for the two- and three-level case, respectively. It is easily seen that the number of the suppressed nodes of the spectral envelope indeed increases as compared to the case of $n=1$.

C. Comparison between RWA and non-RWA results

In this section, we discuss the performance of the RWA by comparing its predictions with those of TRWA and variational methods. Let us first address the consistency between the TRWA and RWA results in the weak-coupling limit, where the RWA is expected to be valid. As $\alpha\to 0$, we simply have $\tilde{\Omega}_j\to\Omega_j$ and $W\to 0$. On the

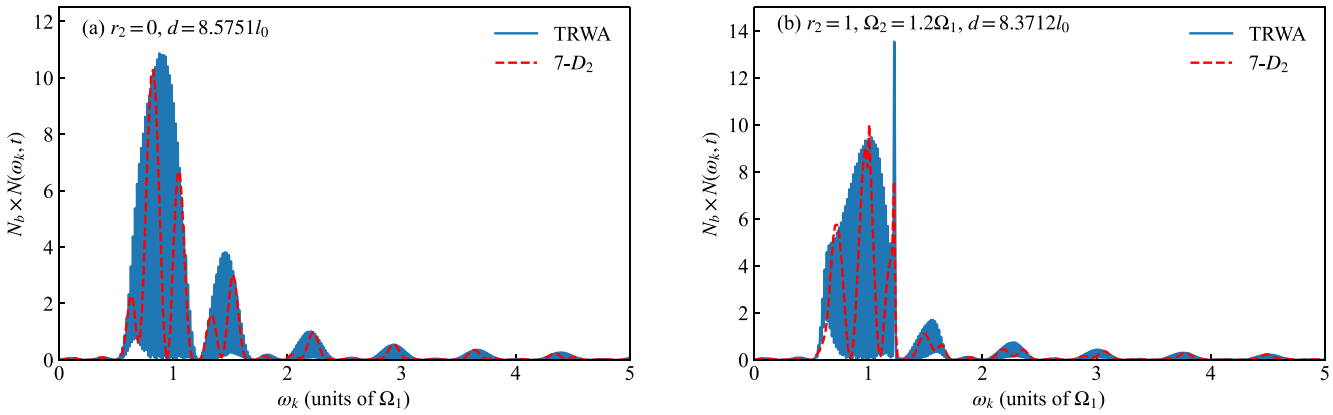

FIG. 6. Emission spectrum in the two-level case (a) and three-level case (b) obtained by multiplying $N(\omega_k, t)|_{t=350\Omega_1^{-1}}$ with N_b for $\alpha = 0.1$, $c_1 = 1$, $c_2 = 0$, $N_c = 3$, and $n = 4$. The values of d in panels (a) and (b) are obtained from Eqs. (42) and (45), respectively. $N_b = 3000$ is used for the TRWA method and $N_b = 300$ for the variational method.

other hand, in the weak-coupling limit, the emission spectrum is very narrow because the decay rate is much smaller than its transition frequency. That is to say, only the modes nearly resonant with the atom contribute significantly and we simply have $\tilde{\lambda}_{kj} \to \frac{r_j \bar{\lambda}_k}{2}$. Consequently, in the weak-coupling limit, the TRWA Hamiltonian naturally reduces to the RWA Hamiltonian. This means that the TRWA results become consistent with the RWA results in the weak-coupling limit.

Although the RWA and TRWA methods are in agreement with each other in the weak-coupling limit, they become inconsistent in a strong-coupling regime. Let us exemplify the difference between the RWA and non-RWA theories in the two-level case. Figure 7 shows the emission spectra and dynamics obtained from the three methods for $c_1 = 1$, $c_2 = 0$, $r_2 = 0$, $N_c = 3$, and the three pairs of (α, d). We note that, as α increases, the deviation between the TRWA and RWA results becomes more and more apparent, while the TRWA results are in agreement with the variational results. This indicates the inadequacy of the RWA and the important role of the counter-rotating terms in a strong coupling regime. The dramatic difference between the RWA and non-RWA results is simply ascribed to the fact that a bound state is formed in the non-RWA case while there are no bound states in the RWA case. In other words, the RWA and non-RWA theories give rise to different conditions for the formation of the bound states in a strong coupling regime. Similarly, the RWA is no longer valid for the V-type three-level giant atom in a strong-coupling regime.

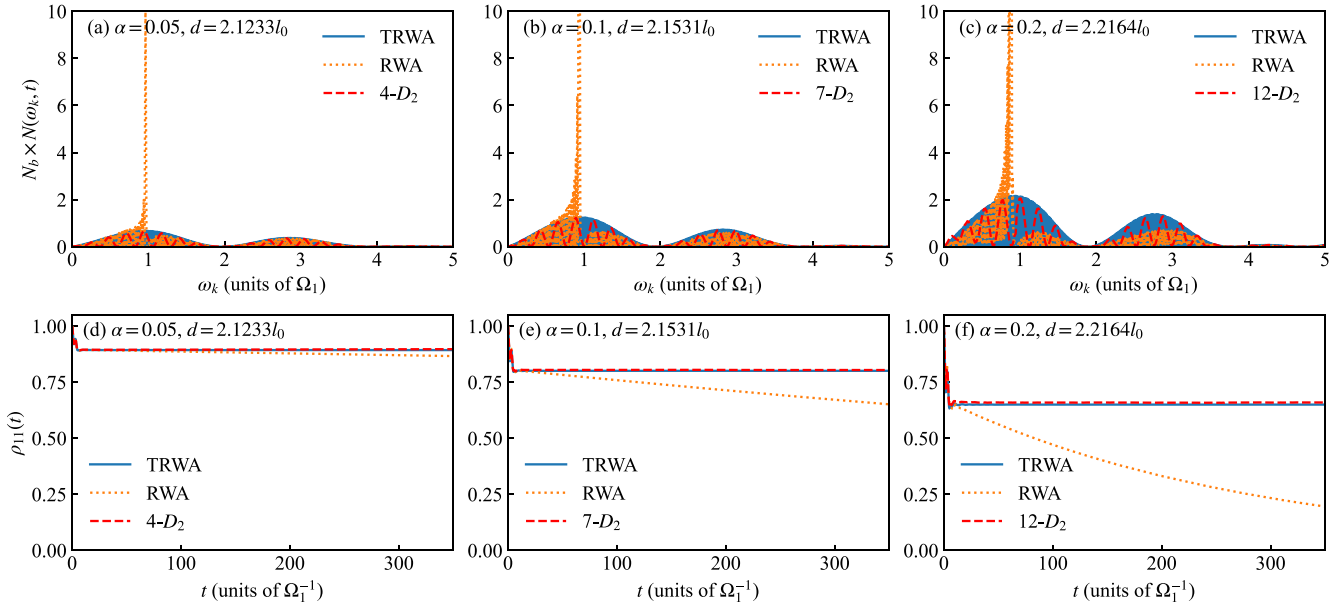

FIG. 7. (a)–(c) Emission spectrum in the two-level case obtained by multiplying $N(\omega_k, t)|_{t=350\Omega_1^{-1}}$ with N_b for $c_1 = 1$, $c_2 = 0$, $r_2 = 0$, $N_c = 3$, and the three pairs of (α, d). The values of d are obtained from Eq. (42) with $n = 1$. (d)–(f) Dynamics of excited-state population calculated by the TRWA, RWA, and variational methods for the parameters in (a)–(c). $N_b = 3000$ is used for the TRWA and RWA methods, and $N_b = 300$ for the variational method.

IV. CONCLUSIONS

In summary, we have studied the spontaneous emission spectra of a few-level giant atom strongly coupled to a one-dimensional waveguide by employing the TRWA and variational methods, which are beyond the RWA and the Markovian approximation. The two methods are found to be consistent with each other in a strong-coupling regime. We have illustrated that the suppression of the spontaneous emission in either two-level or three-level giant atoms can be realized by using two different protocols. One is to use the zeros of the function $F(\omega)$, which makes it possible to suppress spontaneous emission at certain frequencies by tuning the distance between the few coupling points. The other is to use the formation of bound states, which suppresses the total intensity of the spontaneous emission. The underlying cause of both protocols is the destructive interference effects arising from the multiple coupling points, which result in dark lines. The present results offer insights into the spectral features of a few-level giant atom in a strong-coupling regime and show the possibility of suppressing the spontaneous emission by designing the configuration of the multiple coupling points.

ACKNOWLEDGMENT

Support from the National Natural Science Foundation of China (Grants No. 12005188 and No. 11774226) is gratefully acknowledged.

APPENDIX A: DERIVATION OF THE POPULATION OF THE GIANT ATOM

The population in the laboratory frame can be calculated in terms of a_{j0} and a_{0k} by taking account of the unitary transformation as follows:

$$\begin{aligned}\rho_{jj}(t) &= \langle\Psi(0)|e^{iHt}|j\rangle\langle j|e^{-iHt}|\Psi(0)\rangle \\ &= \langle\Psi'(0)|e^{iH't}e^{S}|j\rangle\langle j|e^{-S}e^{-iH't}|\Psi'(0)\rangle \\ &\approx \langle\Psi'(t)|\big\{|j\rangle\langle j| + [S,|j\rangle\langle j|] \\ &\quad + \tfrac{1}{2}[S,[S,|j\rangle\langle j|]]\big\}|\Psi'(t)\rangle, \end{aligned} \tag{A1}$$

where $|\Psi'(t)\rangle = e^{-iH't}|\Psi'(0)\rangle$ is a solution of Eq. (17). To arrive at Eq. (21), we further neglect the normally ordered double bosonic operators in $\frac{1}{2}[S,[S,|j\rangle\langle j|]]$, which contributes insignificantly when the atom-field interaction is moderately weak and in the single-excitation case. If we replace $|j\rangle\langle j|$ in Eq. (A1) with $b_k^\dagger b_k$, a similar calculation leads to the photon number in the k mode, i.e., Eq. (22) in the main text.

APPENDIX B: LAPLACE TRANSFORMS OF THE EQUATIONS OF MOTION

Using the initial conditions $a_{j0}|_{t=0} = c_j$ and $a_{0k}|_{t=0} = 0$, we simply have the Laplace transforms of a_{j0} $(j = 1, 2)$ and a_{0k} for the equations of motion (17) as follows:

$$\bar{a}_{10} = \frac{ic_1[ip - \tilde{\Omega}_2 - R_{22}(ip)] - ic_2[W - R_{12}(ip)]}{[ip - \tilde{\Omega}_1 - R_{11}(ip)][ip - \tilde{\Omega}_2 - R_{22}(ip)] - [W - R_{12}(ip)][W - R_{21}(ip)]}, \tag{B1}$$

$$\bar{a}_{20} = \frac{ic_2[ip - \tilde{\Omega}_1 - R_{11}(ip)] - ic_1[W - R_{21}(ip)]}{[ip - \tilde{\Omega}_1 - R_{11}(ip)][ip - \tilde{\Omega}_2 - R_{22}(ip)] - [W - R_{12}(ip)][W - R_{21}(ip)]}, \tag{B2}$$

$$\bar{a}_{0k} = \sum_{j=1}^{2} \frac{\tilde{\lambda}_{kj}^* \bar{a}_{j0}}{ip - \tilde{\Omega}_0 - \omega_k}, \tag{B3}$$

where

$$R_{jj'}(z) = \sum_p \frac{\tilde{\lambda}_{pj}\tilde{\lambda}_{pj'}^*}{z - \tilde{\Omega}_0 - \omega_p}. \tag{B4}$$

The inversion of the Laplace transforms yields

$$a_{10} = \frac{1}{2\pi i}\int_{+\infty}^{-\infty} \frac{c_1\tilde{A}_2(\omega) - c_2\tilde{B}(\omega)}{\tilde{A}_1(\omega)\tilde{A}_2(\omega) - \tilde{B}^2(\omega)} e^{-i(\omega+\tilde{\Omega}_0)t} d\omega, \tag{B5}$$

$$a_{20} = \frac{1}{2\pi i}\int_{+\infty}^{-\infty} \frac{c_2\tilde{A}_1(\omega) - c_1\tilde{B}(\omega)}{\tilde{A}_1(\omega)\tilde{A}_2(\omega) - \tilde{B}^2(\omega)} e^{-i(\omega+\tilde{\Omega}_0)t} d\omega, \tag{B6}$$

where $\tilde{A}_j(\omega)$ and $\tilde{B}(\omega)$ are defined in the main text. Although the above integrals are difficult to be analytically calculated, they give insights into the properties of the long-time behaviors of the excited states. Note that if the fractional functions in the integrals are bounded, a_{j0} should be trivially vanishing as $t \to \infty$ due to the oscillatory nature of the exponential function. Nonvanishing values of a_{j0} can only be expected if there are some singularities in real axis for the fractional functions, which causes the integrands to be unbounded. In this scenario, we have the condition for nonvanishing a_{j0}, that is,

$$\tilde{A}_1(\omega)\tilde{A}_2(\omega) - \tilde{B}^2(\omega) = 0 \tag{B7}$$

holds for a purely real ω. This equation turns out to have real solutions in a giant-atom model under certain conditions, which physically corresponds to bound states [30,32,46]. Nevertheless, in most cases, the equation has complex-valued solutions with a nonvanishing imaginary part, which means that the excitation has a finite lifetime.

The inversion of $\bar{a}_{0k}$ yields

$$\begin{aligned} a_{0k} = \frac{1}{2\pi i}\int_{+\infty}^{-\infty} d\omega \frac{\exp[-i(\omega+\tilde{\Omega}_0)t]}{\omega + i0^+ - \omega_k} \\ \times \left[\tilde{\lambda}_{k1}^* \frac{c_1\tilde{A}_2(\omega) - c_2\tilde{B}(\omega)}{\tilde{A}_1(\omega)\tilde{A}_2(\omega) - \tilde{B}^2(\omega)}\right. \\ \left. + \tilde{\lambda}_{k2}^* \frac{c_2\tilde{A}_1(\omega) - c_1\tilde{B}(\omega)}{\tilde{A}_1(\omega)\tilde{A}_2(\omega) - \tilde{B}^2(\omega)}\right]. \end{aligned} \tag{B8}$$

Provided Eq. (B7) has complex solutions, we can obtain an analytical expression for a_{0k} in the long-time limit by just considering the simple pole $\omega = \omega_k - i0^+$.

[1] M. O. Scully and M. S. Zubairy, *Quantum Optics* (Cambridge University Press, Cambridge, UK, 1997).

[2] E. M. Purcell, Spontaneous emission probabilities at radio frequencies, in *Confined Electrons and Photons: New Physics and Applications*, edited by E. Burstein and C. Weisbuch (Springer US, Boston, MA, 1995), pp. 839–839.

[3] S.-Y. Zhu and M. O. Scully, Spectral line elimination and spontaneous emission cancellation via quantum interference, Phys. Rev. Lett. **76**, 388 (1996).

[4] A. A. Houck, J. A. Schreier, B. R. Johnson, J. M. Chow, J. Koch, J. M. Gambetta, D. I. Schuster, L. Frunzio, M. H. Devoret, S. M. Girvin, and R. J. Schoelkopf, Controlling the spontaneous emission of a superconducting transmon qubit, Phys. Rev. Lett. **101**, 080502 (2008).

[5] N. M. Sundaresan, Y. Liu, D. Sadri, L. J. Szőcs, D. L. Underwood, M. Malekakhlagh, H. E. Türeci, and A. A. Houck, Beyond strong coupling in a multimode cavity, Phys. Rev. X **5**, 021035 (2015).

[6] R. H. Dicke, Coherence in spontaneous radiation processes, Phys. Rev. **93**, 99 (1954).

[7] N. E. Rehler and J. H. Eberly, Superradiance, Phys. Rev. A **3**, 1735 (1971).

[8] K. Lalumière, B. C. Sanders, A. F. van Loo, A. Fedorov, A. Wallraff, and A. Blais, Input-output theory for waveguide QED with an ensemble of inhomogeneous atoms, Phys. Rev. A **88**, 043806 (2013).

[9] S. Zeeb, C. Noh, A. S. Parkins, and H. J. Carmichael, Superradiant decay and dipole-dipole interaction of distant atoms in a two-way cascaded cavity QED system, Phys. Rev. A **91**, 023829 (2015).

[10] M. Bojer and J. von Zanthier, Dicke-like superradiance of distant noninteracting atoms, Phys. Rev. A **106**, 053712 (2022).

[11] G. Liu, W. Xiong, and Z.-J. Ying, Switchable superradiant phase transition with Kerr magnons, Phys. Rev. A **108**, 033704 (2023).

[12] F. Lohof, D. Schumayer, D. A. W. Hutchinson, and C. Gies, Signatures of superradiance as a witness to multipartite entanglement, Phys. Rev. Lett. **131**, 063601 (2023).

[13] S. Noda, M. Fujita, and T. Asano, Spontaneous-emission control by photonic crystals and nanocavities, Nat. Photon. **1**, 449 (2007).

[14] R. Manenti, A. F. Kockum, A. Patterson, T. Behrle, J. Rahamim, G. Tancredi, F. Nori, and P. J. Leek, Circuit quantum acoustodynamics with surface acoustic waves, Nat. Commun. **8**, 975 (2017).

[15] G. Andersson, B. Suri, L. Guo, T. Aref, and P. Delsing, Non-exponential decay of a giant artificial atom, Nat. Phys. **15**, 1123 (2019).

[16] B. Kannan, M. J. Ruckriegel, D. L. Campbell, A. F. Kockum, J. Braumüller, D. K. Kim, M. Kjaergaard, P. Krantz, A. Melville, B. M. Niedzielski, A. Vepsäläinen, R. Winik, J. L. Yoder, F. Nori, T. P. Orlando, S. Gustavsson, and W. D. Oliver, Waveguide quantum electrodynamics with superconducting artificial giant atoms, Nature (London) **583**, 775 (2020).

[17] A. M. Vadiraj, A. Ask, T. G. McConkey, I. Nsanzineza, C. W. S. Chang, A. F. Kockum, and C. M. Wilson, Engineering the level structure of a giant artificial atom in waveguide quantum electrodynamics, Phys. Rev. A **103**, 023710 (2021).

[18] L. Du, Y. Zhang, J.-H. Wu, A. F. Kockum, and Y. Li, Giant atoms in a synthetic frequency dimension, Phys. Rev. Lett. **128**, 223602 (2022).

[19] A. González-Tudela, C. S. Muñoz, and J. I. Cirac, Engineering and harnessing giant atoms in high-dimensional baths: A proposal for implementation with cold atoms, Phys. Rev. Lett. **122**, 203603 (2019).

[20] S. Longhi, Photonic simulation of giant atom decay, Opt. Lett. **45**, 3017 (2020).

[21] J. Q. You and F. Nori, Atomic physics and quantum optics using superconducting circuits, Nature (London) **474**, 589 (2011).

[22] A. Frisk Kockum, P. Delsing, and G. Johansson, Designing frequency-dependent relaxation rates and lamb shifts for a giant artificial atom, Phys. Rev. A **90**, 013837 (2014).

[23] L. Guo, A. Grimsmo, A. F. Kockum, M. Pletyukhov, and G. Johansson, Giant acoustic atom: A single quantum system with a deterministic time delay, Phys. Rev. A **95**, 053821 (2017).

[24] L. Du, M.-R. Cai, J.-H. Wu, Z. Wang, and Y. Li, Single-photon nonreciprocal excitation transfer with non-Markovian retarded effects, Phys. Rev. A **103**, 053701 (2021).

[25] W. Cheng, Z. Wang, and Y.-X. Liu, Topology and retardation effect of a giant atom in a topological waveguide, Phys. Rev. A **106**, 033522 (2022).

[26] L. Du, Y.-T. Chen, Y. Zhang, and Y. Li, Giant atoms with time-dependent couplings, Phys. Rev. Res. **4**, 023198 (2022).

[27] A. Soro and A. F. Kockum, Chiral quantum optics with giant atoms, Phys. Rev. A **105**, 023712 (2022).

[28] A. Soro, C. S. Muñoz, and A. F. Kockum, Interaction between giant atoms in a one-dimensional structured environment, Phys. Rev. A **107**, 013710 (2023).

[29] L. Du, Y.-T. Chen, Y. Zhang, Y. Li, and J.-H. Wu, Decay dynamics of a giant atom in a structured bath with broken time-reversal symmetry, Quantum Sci. Technol. **8**, 045010 (2023).

[30] S. Guo, Y. Wang, T. Purdy, and J. Taylor, Beyond spontaneous emission: Giant atom bounded in the continuum, Phys. Rev. A **102**, 033706 (2020).

[31] W. Zhao and Z. Wang, Single-photon scattering and bound states in an atom-waveguide system with two or multiple coupling points, Phys. Rev. A **101**, 053855 (2020).

[32] L. Guo, A. F. Kockum, F. Marquardt, and G. Johansson, Oscillating bound states for a giant atom, Phys. Rev. Res. **2**, 043014 (2020).

[33] L. Du and Y. Li, Single-photon frequency conversion via a giant Λ-type atom, Phys. Rev. A **104**, 023712 (2021).

[34] S. L. Feng and W. Z. Jia, Manipulating single-photon transport in a waveguide-QED structure containing two giant atoms, Phys. Rev. A **104**, 063712 (2021).

[35] X.-L. Yin, Y.-H. Liu, J.-F. Huang, and J.-Q. Liao, Single-photon scattering in a giant-molecule waveguide-QED system, Phys. Rev. A **106**, 013715 (2022).

[36] Y.-T. Chen, L. Du, L. Guo, Z. Wang, Y. Zhang, Y. Li, and J.-H. Wu, Nonreciprocal and chiral single-photon scattering for giant atoms, Commun. Phys. **5**, 215 (2022).

[37] J. Zhou, X.-L. Yin, and J.-Q. Liao, Chiral and nonreciprocal single-photon scattering in a chiral-giant-molecule waveguide-QED system, Phys. Rev. A **107**, 063703 (2023).

[38] X. Li, W. Zhao, and Z. Wang, Controlling photons by phonons via giant atom in a waveguide QED setup, Opt. Lett. **48**, 3595 (2023).

[39] A. F. Kockum, G. Johansson, and F. Nori, Decoherence-free interaction between giant atoms in waveguide quantum electrodynamics, Phys. Rev. Lett. **120**, 140404 (2018).

[40] L. Du, L. Guo, and Y. Li, Complex decoherence-free interactions between giant atoms, Phys. Rev. A **107**, 023705 (2023).

[41] H. Yu, Z. Wang, and J.-H. Wu, Entanglement preparation and nonreciprocal excitation evolution in giant atoms by controllable dissipation and coupling, Phys. Rev. A **104**, 013720 (2021).

[42] X.-L. Yin, W.-B. Luo, and J.-Q. Liao, Non-markovian disentanglement dynamics in double-giant-atom waveguide-QED systems, Phys. Rev. A **106**, 063703 (2022).

[43] X.-L. Yin and J.-Q. Liao, Generation of two-giant-atom entanglement in waveguide-QED systems, Phys. Rev. A **108**, 023728 (2023).

[44] A. C. Santos and R. Bachelard, Generation of maximally entangled long-lived states with giant atoms in a waveguide, Phys. Rev. Lett. **130**, 053601 (2023).

[45] D. D. Noachtar, J. Knörzer, and R. H. Jonsson, Nonperturbative treatment of giant atoms using chain transformations, Phys. Rev. A **106**, 013702 (2022).

[46] S. Terradas-Briansó, C. A. González-Gutiérrez, F. Nori, L. Martín-Moreno, and D. Zueco, Ultrastrong waveguide QED with giant atoms, Phys. Rev. A **106**, 063717 (2022).

[47] H. Zheng, S. Y. Zhu, and M. S. Zubairy, Quantum zeno and anti-zeno effects: Without the rotating-wave approximation, Phys. Rev. Lett. **101**, 200404 (2008).

[48] A. Klimov and S. Chumakov, *A Group-Theoretical Approach to Quantum Optics* (Wiley-VCH, Weinheim, 2009).

[49] Z.-H. Li, D.-W. Wang, H. Zheng, S.-Y. Zhu, and M. S. Zubairy, Quantum interference due to energy shifts and its effect on spontaneous emission, Phys. Rev. A **82**, 050501(R) (2010).

[50] D.-W. Wang, Z.-H. Li, H. Zheng, and S.-Y. Zhu, Time evolution, lamb shift, and emission spectra of spontaneous emission of two identical atoms, Phys. Rev. A **81**, 043819 (2010).

[51] Y. B. Dong, Z. H. Li, Y. Li, and S.-Y. Zhu, Effect of the third level on time evolution of the spontaneous upper level decay due to counter-rotating terms, Phys. Rev. A **85**, 013832 (2012).

[52] T. Deng, Y. Yan, L. Chen, and Y. Zhao, Dynamics of the two-spin spin-Boson model with a common bath, J. Chem. Phys. **144**, 144102 (2016).

[53] M. Werther and F. Großmann, Apoptosis of moving nonorthogonal basis functions in many-particle quantum dynamics, Phys. Rev. B **101**, 174315 (2020).

[54] Y. Zhao, K. Sun, L. Chen, and M. Gelin, The hierarchy of Davydovs Ansätze and its applications, WIREs Comput. Mol. Sci. **12**, e1589 (2022).

[55] Y. Zhao, The hierarchy of davydov's ansätze: From guesswork to "numerically exact" many-body wave functions, J. Chem. Phys. **158**, 080901 (2023).

[56] P. Forn-Díaz, J. J. García-Ripoll, B. Peropadre, J.-L. Orgiazzi, M. A. Yurtalan, R. Belyansky, C. M. Wilson, and A. Lupascu, Ultrastrong coupling of a single artificial atom to an electromagnetic continuum in the nonperturbative regime, Nat. Phys. **13**, 39 (2017).

[57] P. Forn-Díaz, L. Lamata, E. Rico, J. Kono, and E. Solano, Ultrastrong coupling regimes of light-matter interaction, Rev. Mod. Phys. **91**, 025005 (2019).

[58] A. F. Kockum, A. Miranowicz, S. D. Liberato, S. Savasta, and F. Nori, Ultrastrong coupling between light and matter, Nat. Rev. Phys. **1**, 19 (2019).

[59] Y. Yan, Spontaneous emission spectrum from a V-type artificial atom in a strong-coupling regime: Dark lines and line narrowing, Phys. Rev. A **108**, 043712 (2023).

[60] J. Frenkel, *Wave Mechanics* (Oxford University Press, Oxford, 1934).

[61] N. Zhou, L. Chen, Z. Huang, K. Sun, Y. Tanimura, and Y. Zhao, Fast, accurate simulation of polaron dynamics and multidimensional spectroscopy by multiple Davydov trial states, J. Phys. Chem. A **120**, 1562 (2016).

[62] L. Wang, Y. Fujihashi, L. Chen, and Y. Zhao, Finite-temperature time-dependent variation with multiple Davydov states, J. Chem. Phys. **146**, 124127 (2017).

[63] L. Zhang, L. Wang, M. F. Gelin, and Y. Zhao, Dynamics of dissipative Landau-Zener transitions in an anisotropic three-level system, J. Chem. Phys. **158**, 204115 (2023).

[64] S.-Y. Zhu, R. C. F. Chan, and C. P. Lee, Spontaneous emission from a three-level atom, Phys. Rev. A **52**, 710 (1995).